NASA TM-87725

NASA Technical Memorandum 87725 NASA-TM-87725 19860017175

BOUNDARY FORCE METHOD FOR ANALYZING TWO-DIMENSIONAL CRACKED BODIES

P. W. Tan, I. S. Raju, and J. C. Newman, Jr.

May 1986

National Aeronautics and
Space Administration

Langley Research Center
Hampton, Virginia 23665

SUMMARY

The Boundary Force Method (BFM) was formulated for the two-dimensional stress analysis of complex crack configurations. In this method, only the boundaries of the region of interest are modeled. The boundaries are divided into a finite number of straight-line segments, and at the center of each segment, concentrated forces and a moment are applied. This set of unknown forces and moments are calculated to satisfy the prescribed boundary conditions of the problem. The elasticity solution for the stress distribution due to concentrated forces and a moment applied at an arbitrary point in a cracked infinite plate are used as the fundamental solution. Thus, the crack need not be modeled as part of the boundary.

The formulation of the BFM is described and the accuracy of the method is established by analyzing several crack configurations for which accepted stress-intensity factor solutions are known. The crack configurations investigated include mode I and mixed mode (mode I and II) problems. The results obtained are, in general, within ±0.5 percent of accurate numerical solutions.

The versatility of the method is demonstrated through the analysis of complex crack configurations for which limited or no solutions are known.

INTRODUCTION

Damage tolerant design criteria for structural members require the ability to predict crack-growth rates and fracture strengths. In these predictions, stress-intensity factors are the most important parameters. Therefore, for accurate predictions, accurate stress-intensity factors are needed.

In two-dimensional analyses, many methods have been used to determine stress concentration factors for holes or notches and stress-intensity factors for cracks. Three of the most popular numerical methods are the Finite Element Method (FEM), the Boundary Collocation Method and the Boundary Element Method (BEM).

The FEM has enjoyed wide-spread use in the last three decades. However, in the field of fracture mechanics, FEM is cumbersome to use. In the finite element approach, relatively large numbers of elements are needed to accurately model the crack region and, for complex configurations with cracks and notches, the number of elements needed to accurately model these problems can be extremely large. (Thus, a correspondingly large effort is required to construct such a model.) Moreover, in crack-growth-rate predictions, stress-intensity factors must be found for various crack lengths. Since a new mesh must be generated for each new crack length to accurately model the crack tip, a large amount of time is needed in the FEM for modeling.

In the collocation method, only the boundaries of the region of interest need to be modeled. Compared to the FEM, where the entire region must be modeled, the collocation method presents an attractive alternative. In this technique however, the basic stress functions need to be changed for different classes of problems. Therefore in the collocation method, a large amount of time can be spent in developing and formulating new stress functions for each class of problems.

With the BEM, only the boundaries of the region of interest are modeled. The boundaries are discretized into a series of line segments. In this paper, a more general method, the Boundary Force Method (BFM), is formulated. The BFM is a form of an indirect BEM that models only the boundaries as in the collocation method, but does not require different stress functions for different classes of problems. Before presenting the details of the BFM, a brief description of previous work in indirect boundary element methods related to the BFM is presented.

One of the earliest indirect formulations of BEM by Nisitani [1] was called the "body force" method. In his method, the unknowns were constant body force densities in the x- and y-directions applied on each segment of the discretized boundaries. The boundary conditions were satisfied in terms of tractions. For cracked bodies, the crack was also modeled as a very slender elliptical notch [2-4].

Isida [5] improved on the accuracy of the body force method by satisfying the boundary conditions in terms of resultant forces. The unknowns in his technique were the body force densities in the x- and y-directions on each segment of the discretized boundaries. Again, cracks were modeled as very slender elliptical notches.

Erdogan and Arin [6] introduced a boundary method to analyze an elastic domain containing a crack. The stress-free conditions on the crack faces were satisfied exactly by using the analytical solution for concentrated forces in an infinite plate with a crack. Thus, the crack faces did not have to be modeled. The unknowns in this analysis were the concentrated forces in the x- and y-directions applied again on the boundaries.

In the present BFM, the stress-free conditions on the crack faces are exactly satisfied by using Erdogan's analytical solution for concentrated forces and a moment in an infinite plate with a crack [7], thus, eliminating the need to model the crack. The unknowns in the BFM are the concentrated forces in the x- and y-directions and a moment on each segment of the discretized boundaries.

Briefly, the essential differences among the methods of Nisitani [1], Isida [5], Erdogan and Arin [6] and the present BFM can be grouped in three categories: the fundamental solutions, the treatment of the boundary conditions, and the treatment of the crack faces. These techniques and their differences are summarized in Table 1.

In this paper, first the formulation of the BFM is presented and the fundamental solution is briefly reviewed. Studies were performed on a center cracked and a single-edge cracked specimen to investigate the rate of convergence of the BFM. The accuracy of the BFM was established by analyzing crack configurations for which accurate numerical solutions are known. These were a crack between two circular holes in an infinite plate and a slant single-edge crack in a finite plate subjected to uniaxial tension. To demonstrate the versatility and "ease of use", the BFM was also used to obtain stress-intensity factor solutions for two crack configurations for which very limited or no solutions are available. These were a crack emanating from an semi-circular edge notch and a four-hole cracked specimen subjected to uniaxial tension.

LIST OF SYMBOLS

a	crack length or one-half crack length
C	resultant couple
E	Young's modulus
$[F]$	influence coefficient matrix
F_x, F_y	resultant forces in the x- and y-directions, respectively
H, W	height and width of rectangular plates, respectively
K	stress-intensity factor
L_i	length of segment i
M	concentrated moment
N	number of segments
p_i, q_i, m_i	unit loads and moment on the i^{th} segment
P, Q	concentrated forces in the y- and x-directions, respectively

$\{P\}$	vector of unknown forces and moments
$\{R\}$	externally applied load vector
S	remote applied stress
u, v	displacements in the x- and y-directions, respectively
x, y	Cartesian coordinates
z	complex variable, $z = x + iy$
z_0	location of forces and moment, $z_0 = x_0 + iy_0$
β	angle of inclination of crack
κ	material constant: $= 3-4\nu$ for plane strain $= (3-\nu)/(1+\nu)$ for plane stress
λ_x, λ_y	projection of sub-arc onto the x- and y-axes, respectively
μ	shear modulus
ν	Poisson's ratio
σ_x, σ_y, σ_{xy}	Cartesian stresses
σ_n, σ_{nt}	normal and shear stresses on the boundary
ε_x, ε_y, ε_{xy}	Cartesian strains
ϕ^*, Ω^*, ϕ_0	complex stress functions

ANALYSIS

In this section, first the formulation of the BFM is presented. Next, the fundamental solution for concentrated forces and a moment at an arbitrary point in an infinite plate is summarized. Then a simple and useful numerical method for evaluating some of the influence coefficients is presented.

Formulation

The Boundary Force Method (BFM) is a numerical technique which uses the superposition of a finite number of sets of concentrated forces and moments in an infinite plate to obtain the solution to the boundary-value problem of interest.

The BFM uses the elasticity solution for concentrated forces and a moment in an infinite plate as the fundamental solution. For plates without a crack, Muskhelishvili's solution [9] for a pair of concentrated forces Q, P and a moment M in an infinite plate is used as the fundamental solution. For a plate with a crack, Erdogan's solution [7] for a pair of concentrated forces Q, P and a moment M in an infinite plate with a crack is used as the fundamental solution. With Erdogan's solution [7] the crack faces need not be modeled as part of the boundary since the stress-free conditions on the crack faces are exactly satisfied.

Because the fundamental solution satisfies all the equations of elasticity in the interior, the only remaining conditions to be satisfied are the conditions on the boundary. The given boundary conditions are satisfied by applying sets of concentrated forces and moments along an "imaginary" boundary traced on an infinite plate, corresponding to the actual configuration. The imaginary boundary is discretized into a number of segments. At the center of each segment, a pair of concentrated forces and a moment are applied at a small distance δ away from the imaginary boundary. The magnitudes of the forces and moment on each segment are determined to approximately satisfy the boundary conditions.

To illustrate the method, consider the problem of a finite plate with a crack subjected to uniaxial tension as shown in Figure 1. The solution to this problem is obtained by the superposition of concentrated forces and moments in an infinite plate with a crack as shown in Figure 2. The dashed lines in Figure 2 correspond to the imaginary boundary of the plate shown in Figure 1.

The first step in the BFM is to discretize the imaginary boundary into a finite number of segments. As an example, Figure 2 shows an idealization of 16 segments (4 in each quadrant) on the imaginary boundary. On each segment i, a concentrated force pair P_i, Q_i and a moment M_i are applied at a small distance δ_i on the outward normal from the mid-point of the segment. The distance δ_i was chosen to be one-fourth of the length of the segment i. This offset was used to eliminate the stress singularities in the computation of the stresses on the boundaries.

The concentrated forces P_i, Q_i and moment M_i on the i^{th} segment create resultant forces R_{x_j} in the x-direction and R_{y_j} in the y-direction, and a resultant couple C_j on the j^{th} segment. Thus, the resultant forces and couple for segment j due to the forces and moments on all segments are

$$R_{x_j} = \sum_{i=1}^{16} (F_{x_j p_i} P_i + F_{x_j q_i} Q_i + F_{x_j m_i} M_i)$$

$$R_{y_j} = \sum_{i=1}^{16} (F_{y_j p_i} P_i + F_{y_j q_i} Q_i + F_{y_j m_i} M_i)$$

$$C_j = \sum_{i=1}^{16} (C_{j p_i} P_i + C_{j q_i} Q_i + C_{j m_i} M_i)$$

Here $F_{x_j p_i}$, $F_{y_j p_i}$, $C_{j p_i}$, etc. are called influence coefficients and are defined as follows:

$F_{x_j p_i}$ = force in the x-direction created on the j^{th} segment due to unit load p_i acting in the y-direction on the i^{th} segment

$F_{y_j p_i}$ = force in the y-direction created on the j^{th} segment due to unit load p_i acting in the y-direction on the i^{th} segment

C_{jp_i} = resultant couple created on the j^{th} segment due to unit load p_i acting in the y-direction on the i^{th} segment

with similar definitions for $F_{x_j q_i}$, $F_{y_j q_i}$, C_{jq_i}, $F_{x_j m_i}$, $F_{y_j m_i}$, and C_{jm_i}.

The resultant forces and couples are assumed to act at the center of the corresponding segments. The resultants on all segments can then be written as

$$[F]_{48\times 48}\,\{P\}_{48\times 1} = \{R\}_{48\times 1} \qquad (1)$$

where $[F]$ is the "influence coefficient" matrix, $\{P\}$ is the vector of unknown forces and moments, and $\{R\}$ is the vector of externally applied resultant forces and moments. The influence coefficient matrix $[F]$ can be expressed as

$$[F] = \left[\begin{array}{cc|cc|cc}
F_{x_1p_1}\cdots & F_{x_1p_{16}} & F_{x_1q_1}\cdots & F_{x_1q_{16}} & F_{x_1m_1}\cdots & F_{x_1m_{16}} \\
F_{y_1p_1}\cdots & F_{y_1p_{16}} & F_{y_1q_1}\cdots & F_{y_1q_{16}} & F_{y_1m_1}\cdots & F_{y_1m_{16}} \\
C_{1p_1}\cdots & C_{1p_{16}} & C_{1q_1}\cdots & C_{1q_{16}} & C_{1m_1}\cdots & C_{1m_{16}} \\
\cdots & \cdots & \cdots & \cdots & \cdots & \cdots \\
\cdots & \cdots & \cdots & \cdots & \cdots & \cdots \\
\cdots & \cdots & \cdots & \cdots & \cdots & \cdots \\
F_{x_{16}p_1}\cdots & F_{x_{16}p_{16}} & F_{x_{16}q_1}\cdots & F_{x_{16}q_{16}} & F_{x_{16}m_1}\cdots & F_{x_{16}m_{16}} \\
F_{y_{16}p_1}\cdots & F_{y_{16}p_{16}} & F_{y_{16}q_1}\cdots & F_{y_{16}q_{16}} & F_{y_{16}m_1}\cdots & F_{y_{16}m_{16}} \\
C_{16p_1}\cdots & C_{16p_{16}} & C_{16q_1}\cdots & C_{16q_{16}} & C_{16m_1}\cdots & C_{16m_{16}}
\end{array}\right] \qquad (2)$$

The coefficient matrix [F] is fully populated and non-symmetric.

The external loading on the plate boundaries (uniform stress S in the y-direction at $y = \pm H/2$, see Figure 1) can be replaced with concentrated forces equal to SL_k, where L_k is the length of the k^{th} segment as shown in Figure 3. The forces in the x-direction and the moment on these boundaries are zero. The force pair and moment acting on each segment of the boundaries $x = \pm W/2$ are also zero since these boundaries are stress free. This set of concentrated force pairs and moments forms the load vector {R} on the right-hand side of equation (1) and can be written as

$$\{R\} = \{R_{x_1}, R_{y_1}, C_1, \ldots\ldots R_{x_{16}}, R_{y_{16}}, C_{16}\}$$

$$\{R\} = \{0, 0, 0, \ldots SL_3, \ldots SL_{14}, \ldots 0, 0\}$$

where R_{x_i} = total force in x-direction on the i^{th} segment due to the external tractions

R_{y_i} = total force in y-direction on the i^{th} segment due to the external tractions

C_i = total moment on the i^{th} segment due to the external tractions

Because the influence coefficient matrix [F] and the external applied load vector {R} are known, the unknown force and moment vector {P} can be obtained by solving the system of linear algebraic simultaneous equations. This set of forces P_i, Q_i and M_i, acting on the imaginary boundary in the infinite plate (see Figure 2), will approximately satisfy the specified boundary conditions. Therefore, the stress state within the region bounded by the imaginary boundary is approximately equal to the stress state in the interior of the finite cracked plate. The stresses and displacements at any point within the plate and the stress-intensity factors at the crack tips can be computed with the system of forces P_i, Q_i and moment M_i ($i = 1$ to 16). A more detailed formulation of the BFM and the advantages of considering symmetry are given in [10].

Fundamental Solution

The BFM formulation uses the elasticity solution for a pair of concentrated forces and a moment in an infinite plate with a crack. Such a solution was formulated by Erdogan [7] for linear, isotropic and homogeneous materials. The solution is presented in Appendix A.

Influence Coefficient Calculations

The influence coefficients in equation (2) are the resultant forces and moment on segment j due to unit forces and moment applied to segment i and are calculated using numerical integration of stresses given in equation (A.2). While the force resultants on the j^{th} segment due to unit loads p_i, q_i and moment m_i on the i^{th} segment are easily obtained in closed form from equation (A.4), the moment resultants C_{jp_i}, C_{jq_i} and C_{jm_i} caused some difficulty, since the resultant moment terms C_{jp_i}, C_{jq_i} and C_{jm_i} can be obtained in closed form only by double integrations of the stress functions. However, after the first integration, the resulting functions consist of a long series of multivalued terms. Hence, a second integration of these functions would be unwieldy and cumbersome, if not impractical. For this reason, the resultant moment C, created by concentrated forces and moment in an infinite plate, is approximated by dividing each segment into two or more parts, and computing the resultant forces on each subdivision. These resultant forces are then multiplied by the corresponding moment arm about the center of the segment. For example, consider a unit load p_1 acting at z_0 in an infinite plate as shown in Figure 4. The segment j, between z_1 and z_2, is divided into two parts ($k = 1$ and 2). The resultant forces created by the unit load p_1 at z_0, along each sub-arc k, are $F^k_{x_j p_1}$ and $F^k_{y_j p_1}$ in the x- and y-directions, respectively. Thus, the resultant couple C_{jp_1} across the j^{th} segment between z_1 and z_2, due to the unit load p_1, is

$$C_{jp_i} = \sum_{k=1}^{2} \left(F^k_{x_j p_1} \lambda^k_{y_j} + F^k_{y_j p_1} \lambda^k_{x_j} \right) \tag{3}$$

where the influence coefficients $F_{x_j p_1}$ and $F_{y_j p_1}$ were defined above and the superscript k refers to the k^{th} subdivision. The terms

λ^k_j = x-distance from the center of the k^{th} subdivision to the center of the j^{th} segment

λ^k_j = y-distance from the center of the k^{th} subdivision to the center of the j^{th} segment

as shown in Figure 4.

The resultant couples C_{jq_i} and C_{jm_i}, due to unit load force q_i and unit moment m_i, can be obtained in a similar fashion.

The accuracy of the coefficients C_{jp_i} increases as the number of the subdivisions k becomes large. From numerical convergence studies on several C_{jp_i}, C_{jq_i} and C_{jm_i} coefficients, a value of $k = 4$ was found to be sufficient in most cases. This numerical procedure simplified the computations considerably and reduced the tedious integrations and cumbersome algebraic manipulations.

RESULTS AND DISCUSSION

First, the accuracy of the BFM is compared with some other boundary methods, where only forces are used as the unknowns, and the convergence characteristics of the BFM are studied by applying the method to two standard crack configurations. Then the BFM is used to analyze mode I and mixed mode problems for which accurate solutions are available in the literature. Finally, the method is used to obtain stress-intensity factor solutions for complex crack configurations for which no solutions are available.

Accuracy and Convergence Studies

In previous boundary methods [1-6], the boundary conditions were satisfied in terms of tractions or resultant forces alone. In the BFM, the boundary conditions are satisfied in terms of resultant forces and moments. The BFM, therefore, has an additional degree of freedom per segment compared to previous boundary methods. To compare the accuracy obtained by satisfying the boundary conditions in terms of resultant forces and moments to that of resultant forces only, a simple configuration was analyzed using the two methods. A center cracked plate with a long crack ($2a/W = 0.8$) was analyzed. Because of symmetry in the problem, only one quarter of the plate was modeled using equal size segments. The relative error in the stress-intensity factors is used for comparison, where the relative error is defined as

$$\text{Relative error} = \left| \frac{K_{computed} - K_{ref}}{K_{ref}} \right|$$

$K_{computed}$ is the stress-intensity factor computed by either method and K_{ref} is the reference value taken from the literature.

Figure 5 presents the relative error as a function of the number of degrees of freedom used in the modeling. For the same number of degrees of freedom, the method that includes the moments as unknowns (BFM) yields a solution which is more accurate than the method where only forces are used as unknowns. The improved accuracy can be attributed to better satisfaction of the boundary conditions when the moment is included. Thus, the BFM is expected to yield a more accurate solution and also have a faster convergence rate than methods where only forces are used. In the above example, the present method yields a very accurate solution (within 1% of the reference solution) with as few as 24 degrees of freedom.

Next, the convergence of the BFM is studied by increasing the number of segments in the idealization. The two problems used, for which very accurate solutions are available, were a center cracked specimen and a single edge cracked specimen. As before, the relative error in the stress-intensity factor is used as the convergence parameter.

For the case of the center-crack tension specimen subjected to uniaxial tension as shown in Figure 6, two extreme crack-length-to-width ratios, $2a/W$ = 0.2 and 0.8, were considered. Because of symmetry, only one quarter of the plate was modeled. Again, equal size segments were used in the models. The relative error in the stress-intensity factors as a function of the number of degrees of freedom is presented in Figure 6. For the small crack ($2a/W = 0.2$), the solution converged much faster than for the large crack length ($2a/W$ = 0.8). This trend shows the effects of the external boundaries on the stress-intensity factor. In both cases, as few as 36 degrees of freedom are sufficient to yield a very accurate solution.

Figure 7 shows the convergence of the relative error for the single edge crack specimen subjected to uniaxial tension. Again for this configuration, two extreme crack-length-to-width ratios, a/W of 0.2 and 0.6, were considered. Because of symmetry, only the top half of the plate was modeled. Equal size segments were used on the boundaries. For the short crack (a/W = 0.2), the rate of convergence of the solution is somewhat faster than that for the long crack (a/W = 0.6). For both crack lengths about 72 degrees of freedom are sufficient to yield a very accurate solution (within 1 percent of the reference solution of [11]).

For the two crack configurations just discussed, equal size boundary segments were used. However, modeling with equal size segments is usually not optimal. Large segments could be used in those regions where the stress gradients are not severe while small segments could be used where the stress gradients are severe. Such a graded model could yield solutions which are more accurate with fewer segments than a model with equal size segments. To construct such graded models, a radial-line method for generating the mesh points on the boundaries was developed and is presented in Appendix B. Using a model generated by the radial-line method, a very accurate solution can be found for considerably fewer degrees of freedom [10].

Comparisons With Other Solutions

To establish the accuracy of the BFM, several complex crack configurations for which accurate solutions are available in the literature were analyzed. These configurations can be divided into two categories: opening mode (mode I) problems and mixed mode (mode I and mode II) problems. For both the mode I and mixed mode problems, the radial-line method (see Appendix B) was used to generate the mesh points with the origin of the radial-lines chosen to be at the crack tip. A value of 10 was used for the dividing factor DF.

Mode I problems. Consider a large plate ($H/R = W/R = 64$) with a crack located between two circular holes as shown in Figure 8. The plate is subjected to remote, uniaxial tension. Again, because of symmetry, only one quarter of the plate was modeled using about 40 segments (about 120 degrees of freedom).

The stress-intensity correction factors for a range of crack-length-to-hole-radius ratios are presented in Figure 8. Results calculated by Newman [12] for an infinite plate using the collocation technique are shown for comparison. For all crack lengths considered, the agreement between the BFM results and the collocation results is excellent (within 1 percent). The small difference is probably due to the large, but finite plate used in the present analysis where an infinite plate was used in [12]. In Figure 8, the dashed line at unity represents the limiting solution as the d/R ratio approaches infinity. For larger crack lengths, $a/R > 2.5$, the influence of the holes is negligible. For small a/R values, the crack tips are shielded by the holes and thus the stress intensity factor is much lower than the solution for the plate without holes.

Mixed mode problems. To demonstrate the validity of the BFM for mixed mode problems, the common mixed mode crack problem of a slant single edge crack in a finite plate subjected to uniaxial tension (see Figure 9) was analyzed. Because of lack of symmetries, the complete plate is modeled with 50 segments or 150 degrees of freedom.

Three angles of inclination, $\beta = 45^{\circ}$, 67.5° and 90° were considered. For each angle β, several a/W ratios were considered. Figures 9 and 10 present the mode I and mode II stress-intensity correction factors, respectively, for each of the cases considered. These stress-intensity correction factors are compared with the results obtained by Wilson using collocation techniques [11]. The agreement between the present results and those obtained by Wilson are generally within 0.5 percent except for the mode II stress-intensity corrections factors for $a/W = 0.6$. For this case, the present results are within 1.5 percent of Wilson's solution [11].

New Solutions

In this section, the BFM is applied to two configurations where few or no stress-intensity factor solutions are available, an edge crack emanating from a semi-circular hole and a four-hole crack specimen. The radial-line method was used to generate the mesh points on the boundaries and the crack tip was chosen as the origin of the radial lines. Again a value of 10 was used for the dividing factor DF.

Edge crack emanating from a semi-circular hole. Figure 11 shows an edge crack emanating from a semi-circular hole. Very few solutions for the range of crack lengths considered here are available in the literature. Thus, the solutions given below will add considerably to the available solutions for this crack configuration.

Due to symmetry, only the upper half of the plate was modeled. The stress-intensity correction factors obtained for three values of notch-depth-to-width ratio ($R/W = 0.25$, 0.125 and 0.0625) are presented in Table 2 and Figure 11. In each case, the notch radius R was held constant and the value of W was increased to obtain the desired R/W ratio. For each R/W ratio, the crack length was varied from about 5 to 50 percent of the plate width. For short cracks, the notch boundary had a significant influence on the stress-intensity factor. However, as the crack tip approached the mid-section of the plate, the stress-intensity factor approached the solution for an edge crack without the notch. Thus, the notch boundary had no influence on the stress-intensity factor when the crack is half-way through the plate as shown in Table 2.

Four-hole crack specimen. Stringers are widely used in aircraft structures as stiffening members to retard or arrest propagating cracks. The four-hole crack specimen shown in Figure 12, which simulates the effect of a stringer on a propagating crack, was analyzed. Due to symmetry, only one quarter of the specimen was modeled.

The stress-intensity correction factors obtained for a range of crack length-to-width ratios ($0 < a/W < 0.9$) are presented in Table 3 and Figure 12. The solution for a similar specimen with no holes (a center-crack tension specimen) is also shown in Figure 12 for comparison. The results for the four-hole specimen show that the stress-intensity factor increases (higher than for the center-crack specimen) as the crack tip approaches the inner edge of the hole. However, as the crack tip approaches the center-line of the holes, the stress-intensity factor decreases (lower than for the center-crack specimen) until a minimum value is obtained at about $a/W = 0.55$. Thus, a propagating crack will be retarded or arrested as it approaches the center-line of the holes. This drop in the stress-intensity factor is due to the shielding of the crack tip by the holes from the externally applied stress field.

CONCLUDING REMARKS

The Boundary Force Method (BFM) was formulated for the two-dimensional analysis of complex crack configurations. In this method, the boundaries of the crack configuration were modeled by straight-line segments. At the center of each of the segments, a horizontal force, a vertical force and a moment were applied. These sets of forces and moments are treated as the unknowns in the problem. These unknowns are determined such that the boundary conditions are satisfied approximately along the boundaries of the configuration. The BFM uses the fundamental elasticity solution of a pair of concentrated forces and a moment at an arbitrary point in an infinite plate with a crack. Therefore, the boundary conditions on the crack faces are satisfied exactly and, hence, the crack faces are not modeled as part of the boundary as in previous boundary element methods.

To verify the accuracy of the method, the BFM was used to analyze several crack configurations for which exact or accurate stress-intensity factor solutions are available in the literature. The crack configurations considered included mode I and mixed mode (mode I & II) problems. The method yielded stress-intensity factors which were in excellent agreement with those in the literature for both the mode I and mixed mode problems. Results showed that for the same degree of accuracy, significantly fewer degrees of freedom were required in the BFM with unknown forces and moments compared to unknown forces only. In general, about 150 degrees of freedom were required to obtain very accurate solutions to complex crack configurations with the BFM with unknown forces and moments.

The versatility of the BFM was demonstrated by analyzing two complex crack configurations for which limited or no solutions are available, an edge crack emanating from a semi-circular hole and the four-hole crack specimen. For each configuration, several crack length-to-width ratios were analyzed and stress-intensity factors are presented. For each configuration, the stress-intensity factors for several crack lengths were obtained with minimal modeling effort since only the boundaries were modeled.

APPENDIX A - FUNDAMENTAL SOLUTION

The BFM formulation uses the elasticity solution for a pair of concentrated forces and a moment in an infinite plate with a crack. Such a solution was formulated by Erdogan [7] for linear, isotropic and homogeneous materials. The solution is presented below.

Stress Functions

Consider an infinite plate with a crack subjected to concentrated forces Q, P and a moment M at an arbitrary point $z_0 = x_0 + iy_0$ as shown in Figure A.1. The complex variable stress functions [7] are

$$\phi^*(z) = -\frac{S}{z - z_0} + \phi_0(z)$$

$$\Omega^*(z) = \frac{\kappa S}{z - \bar{z}_0} + \frac{\bar{S}(\bar{z}_0 - z_0) + im}{(z - \bar{z}_0)^2} + \phi_0(z)$$

$$\phi_0(z) = \frac{1}{2\pi\sqrt{z^2 - a^2}} \left\{ \frac{S}{z - z_0} [I(z) - I(z_0)] \right. \tag{A.1}$$

$$- \frac{\kappa S}{z - \bar{z}_0} [I(z) - I(\bar{z}_0)]$$

$$\left. - [\bar{S}(\bar{z}_0 - z_0) + im][\frac{I(z) - I(\bar{z}_0)}{(z - \bar{z}_0)^2} - \frac{J(\bar{z}_0)}{z - \bar{z}_0}] \right\}$$

where $m = \frac{M}{2\pi}$

$$I(z) = \pi[\sqrt{z^2 - a^2} - z]$$

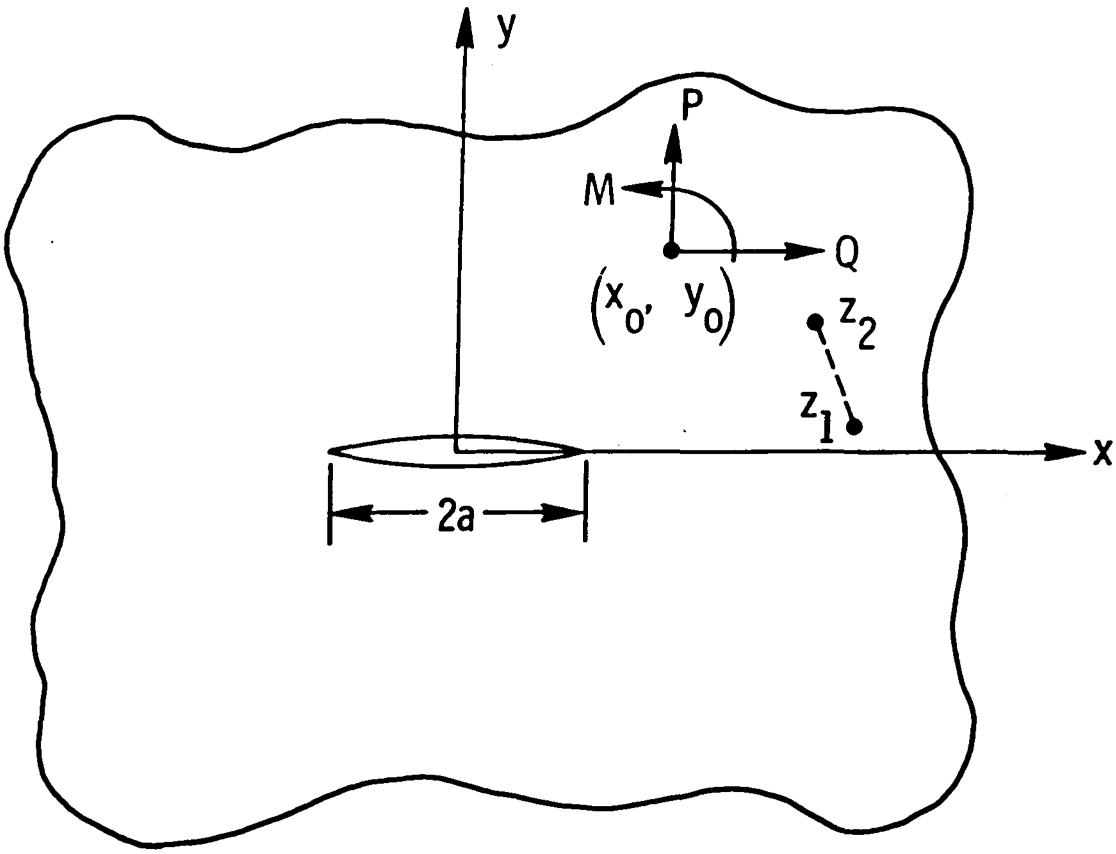

Figure A.1 - Concentrated loads and moment in an infinite plate with a crack.

$$I(z_0) = \pi[\sqrt{z_0^2 - a^2} - z_0]$$

$$J(\bar{z}_0) = \pi\left[\frac{\bar{z}_0}{\sqrt{\bar{z}_0^2 - a^2}} - 1\right]$$

$$S = \frac{Q + iP}{2\pi(1 + \kappa)}$$

Stresses

The stresses at any point, $z = x + iy$, are obtained from the stress functions as

$$\begin{aligned} \sigma_x + \sigma_y &= 2[\phi^*(z) + \overline{\phi^*(z)}] \\ \sigma_y - \sigma_x + i2\sigma_{xy} &= 2[(\bar{z} - z)\phi^{*'}(z) - \phi^*(z) + \bar{\Omega}^*(z)] \end{aligned} \tag{A.2}$$

where the barred quantities are the complex conjugates and the primed quantities represent the derivatives with respect to z. From equations (A.1) and (A.2), the stresses are singular at the concentrated load, that is, the stresses become infinite as z approaches z_0. In addition, the stresses also become infinite as z approaches $\pm a$, the stresses have the required square root singularity at the crack tips, and the stresses vanish as $r \rightarrow \infty$.

Displacements, Forces and Moments

The displacements u and v at any point, $z = x + iy$, are obtained from the stress functions as

$$2\mu(u + iv) = \kappa \int_0^z \phi^*(z)dz - \int_0^{\bar{z}} \Omega^*(\bar{z})d\bar{z} - (z - \bar{z})\overline{\phi^*(z)} \tag{A.3}$$

where μ is the shear modulus. The resultant forces F_x, F_y and the resultant moment M_o across the arc z_1 to z_2 (see Figure A.1) due to the concentrated forces (Q, P) and moment M can be obtained either by integrating the stresses in equation (A.2) from z_1 to z_2, or by using the stress functions in the the following equations:

$$F_x + iF_y = -i[\int\phi^*(z)dz + \int\Omega^*(\bar{z})d\bar{z} + (z - \bar{z})\,\overline{\phi^*(z)}]\Big|_{z_1}^{z_2} \qquad (A.4)$$

$$M_o = \text{Re}\,[\int\int\{\phi(z) + \bar{\Omega}(z)\}dzdz - z\int\{\phi(z) + \bar{\Omega}(z)\}dz + z(z - \bar{z})\phi(z)]\Big|_{z_1}^{z_2} \qquad (A.5)$$

Stress-Intensity Factor

The stress intensity factors for concentrated forces Q and P and moment M applied at an arbitrary point, $z_0 = x_0 + iy_0$, in an infinite plate with a crack (see Figure A.1) are

$$K = K_I + iK_{II} = 2\sqrt{2\pi}\lim_{z\to a}[\sqrt{(z - a)}\;\phi^*(z)]$$

$$= \frac{1}{2\sqrt{\pi a}}\frac{1}{(1 + \kappa)}\Big\{(Q + iP)\Big[\Big(\frac{a + z_0}{\sqrt{z^2 - a^2}} - 1\Big) - \kappa\Big(\frac{a + \bar{z}_0}{\bar{z}^2 - a^2} - 1\Big)\Big] + \frac{a[(Q - iP)(\bar{z}_0 - z_0) + i(1 + \kappa)M]}{(\bar{z}_0 - a)\sqrt{\bar{z}_0^2 - a^2}}\Big\} \qquad (A.6)$$

APPENDIX B - RADIAL LINE METHOD

This appendix describes a systematic procedure, called the radial-line method, for modeling the boundaries of a crack configuration. In the BFM, the accuracy of the stress-intensity factor obtained depends on how well the boundary conditions are approximated. Because the boundaries near the crack tip are subjected to higher stress gradients than the boundaries far from the crack tip, smaller segments are needed to accurately model the boundary conditions near the crack tip. Therefore, a radial-line method that will generate smaller line segments on the boundaries near the crack tip and larger line segments on the boundaries away from the crack tip was developed. With the radial-line method of modeling, a significant reduction in the number of degrees of freedom is realized without sacrificing accuracy. This procedure can be best described using the following example.

Consider a center-crack tension specimen with a crack length 2a as shown in Figure B.1. Because of symmetry, only one quarter of the plate needs to be modeled. The boundary of this quadrant can be divided into two sections: Boundary 1 - the vertical line A to B and Boundary 2 - the horizontal line B to C. Because the stress-intensity factor is the quantity of interest here, let the crack tip at $x = a$ be the point from which all radial lines originate. To determine the segment sizes on Boundary 1, first the distance between the origin of the radial lines (the crack tip) and the starting point z_1 (point A) is computed. Label this distance r_1. The size of the first segment (z_1 to z_2) is chosen to be a fraction of the distance r_1. Thus, the distance from z_1 to z_2 is set equal to r_1/DF where DF is referred to as the dividing factor. Because the factor DF is assumed to be known, the distance to point z_2 can be determined. Next, r_2 the distance from the origin of the radial lines (the crack tip) to z_2 is computed. The size of the second segment, z_2 to z_3, is

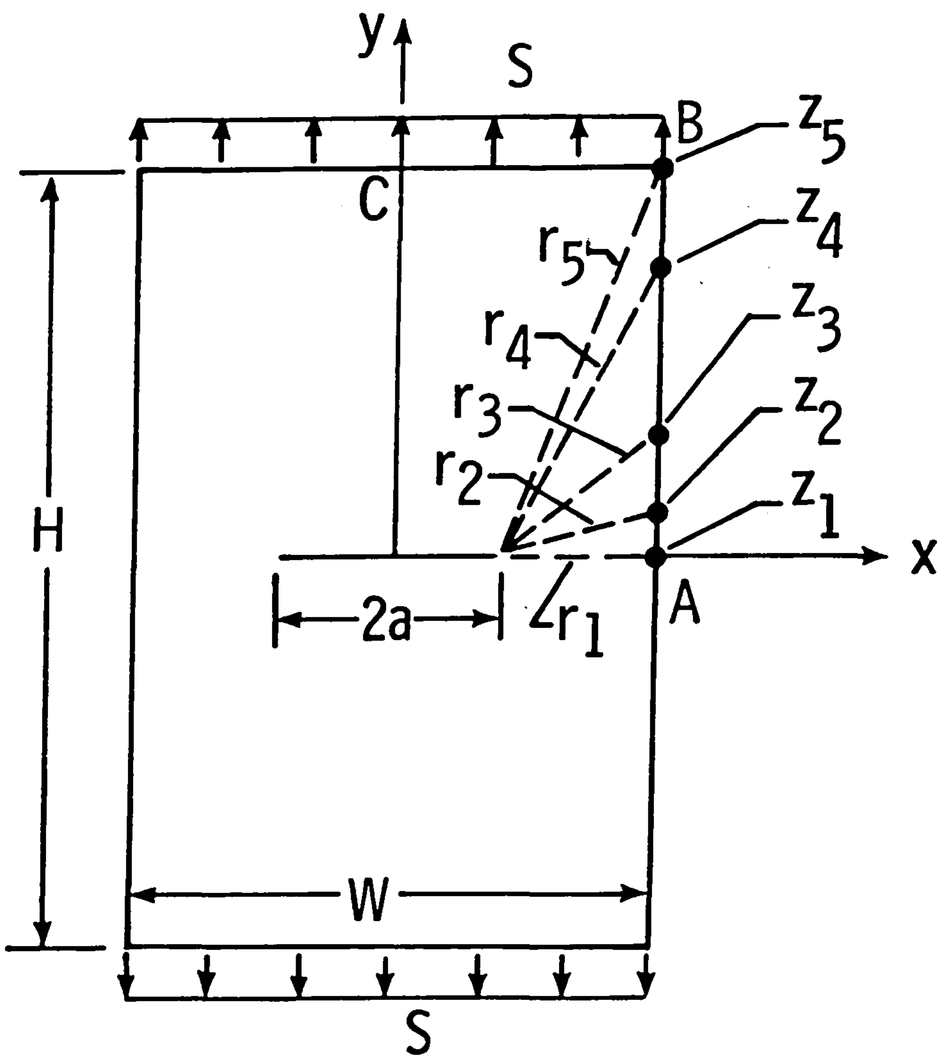

Figure B.1 - Radial-line method for generating mesh points.

a fraction of the distance r_2, so that the size of the second segment is equal to r_2/DF. The dividing factor DF is assumed to be identical throughout the entire modeling. This procedure is repeated until the entire Boundary 1 is discretized. The procedure has to be modified near the end points, such as point B in Figure B.1. If the end point of the last segment exceeds the end point of the boundary (point B), the end point of the boundary is assigned as the end point of the last segment on that boundary. The same radial-line procedure is repeated for Boundary 2 where the starting point of Boundary 2 is the end point of Boundary 1.

In the radial-line method, the size of the segments or the distribution density of the segments is determined by the choice of the origin of the radial line and the value of the dividing factor DF. Both can be chosen arbitrarily. In all the problems investigated in this paper, the origin of the radial-line was chosen to be the crack tip, since the stress-intensity factor is the quantity of interest. A DF value of 10 was used in all the problems.

The most significant advantage of the radial-line method can be demonstrated in the case of a very small crack emanating from a semi-circular notch. Because of the high stress gradient near the crack tip, small segments are needed on portions of the semi-circular boundary nearest the crack tip (see Figure 12). If equal size segments are used, a large number of segments are needed on this curved boundary. However, the portion of the curved boundary that is away from the crack tip does not have high stress gradients and so small size segments on that portion of the boundary are unnecessary. The radial-line method generates small segments near the crack tip and large segments away from the crack tip. This type of modeling will significantly reduce the number of degrees of freedom necessary to model the curve boundary without sacrificing accuracy.

REFERENCES

1. Nisitani, H.: "Two-dimensional problems solved using a digital computer." Journal of Jap. Soc. Mech. Engrs., Vol. 70, No. 580, 1967, pp. 627-635.

2. Nisitani, H.; and Murakami, Y.: "Stress-intensity factors of an elliptical crack or a semi-elliptical crack subject to tension." Int. Journal of Fracture, Vol. 10, No. 3, Sept. 1974, pp. 353-368.

3. Nisitani, H.: "Interference effects among cracks or notches in two-dimensional problems." Int. Conference on Fracture Mechanics and Technology, 1977, Proceedings Vol. 2, pp. 1127-1142.

4. Murakami, Y.; and Nisitani, H.: "A method for calculating stress-intensity factors of an arbitrarily shaped finite plate with a crack." Int. Conference on Fracture Mechanics and Technology, 1977, Proceedings, Vol. 2, pp. 1171-1185.

5. Isida, M.: "A new procedure of the body force method with applications to fracture mechanics." Numerical methods in fracture mechanics; Proceedings of the First International Conferences, Swansea, Wales, Jan. 1978, pp. 81-94.

6. Erdogan, F.; and Arin, K.: "A half plane and a strip with an arbitrarily located crack." Int. Journal of Fracture, Vol. 11, No. 2, 1975, pp. 191-204.

7. Erdogan, F.: "On the stress distribution in a plate with collinear cuts under arbitrary loads." Proc. 4th U. S. National Congress of Applied Mechanics, (1962), pp. 547-553.

8. Timoshenko, S.; and Goodier, J. N.: Theory of Elasticity. McGraw-Hill Book Co., Third Edition, 1970, pp. 127.

9. Muskhelishvili, N. I.: Some Basic Problems of the Mathematical Theory of Elasticity. Noordhoff International Publishing, 2nd Ed., 1977.

10. Tan, P. W.: "The Boundary Force Method for Stress Analysis of Arbitrarily Shaped Plates with Notches and Cracks," D. Sc. Dissertation, George Washington University, 1985.

11. Rooke, D. P.; and Cartwright, D. J.: Compendium of Stress Intensity Factors. The Hillingdon Press, Uxbridge, Middx, 1976.

12. Newman, J. C., Jr.: "An improved method of collocation for the stress analysis of cracked plates with various shaped boundaries." NASA TN D-6376, 1971.

Table 1 - Comparison of various indirect boundary element techniques.

Investigator [Ref.]	Fundamental Solutions Used		Treatment of Crack Faces	Treatment of Boundary Conditions (BC)
	Without Crack	With Crack		
Nisitani [1]	Timoshenko's solution [8] for point load in an infinite plate	Same as without crack	Modeled as a very slender elliptical notch $b/a \rightarrow 0$, b= minor axis, a=major axis	BC are satisfied in terms of stresses
Isida [5]	Kolosov-Muskhelishvili solution [9] for point loads in an infinite plate	Same as without crack	Modeled as a very slender elliptical notch $b/a \rightarrow 0$	BC are satisfied in terms of resultant forces
Erdogan and Arin [6]	Kolosov-Muskhelishvili solution [9] for point loads in an infinite plate	Erdogan's solution [7] for point loads in an infinite plate with a crack	No modeling of the crack faces needed	BC are satisfied in terms of resultant forces
Present Method	Kolosov-Muskhelishvili solution[9] for point loads in an infinite plate	Erdogan's [7] solution for point loads in an infinite plate with a crack	No modeling of the crack faces needed	BC are satisfied in terms of resultant forces and moment

Table 2 - Stress-intensity correction factors for an edge crack emanating from a semi-circular hole.

a/R	F_I(R/W = .25)	F_I(R/W = .125)	F_I(R/W = .0625)
1.04	.8860	.6937	.6431
1.05	.9709	.7612	.7018
1.06	1.0392	.8125	.7527
1.08	1.1531	.8995	.8322
1.10	1.2468	.9665	.8929
1.15	1.4068	1.0819	.9951
1.20	1.5259	1.1546	1.0568
1.30	1.6946	1.2410	1.1234
1.50	1.9648	1.3319	1.1751
1.75	2.3356	1.4144	1.1993
2.00	2.8183(a)	1.5006	1.2273
3.00	------	1.9802	1.3390
4.00	------	2.8189(a)	1.4982
6.00	------	------	1.4982
8.00	------	------	2.8200(a)

(a) These values correspond to an a/W ratio of 0.5.

(b) F_I for single edge crack with a/W = 0.5 is 2.8153 [11].

Table 3 - Stress-intensity correction factors for four-hole crack specimen.

a/W	F_I
0.	1.169
.05	1.174
.10	1.191
.15	1.222
.20	1.268
.25	1.332
.30	1.409
.35	1.480
.375	1.498
.40	1.489
.425	1.446
.45	1.361
.475	1.242
.50	1.108
.525	0.989
.55	0.917
.575	0.904
.60	0.946
.65	1.127
.70	1.342
.75	1.558
.80	1.795
.85	2.105
.90	2.599

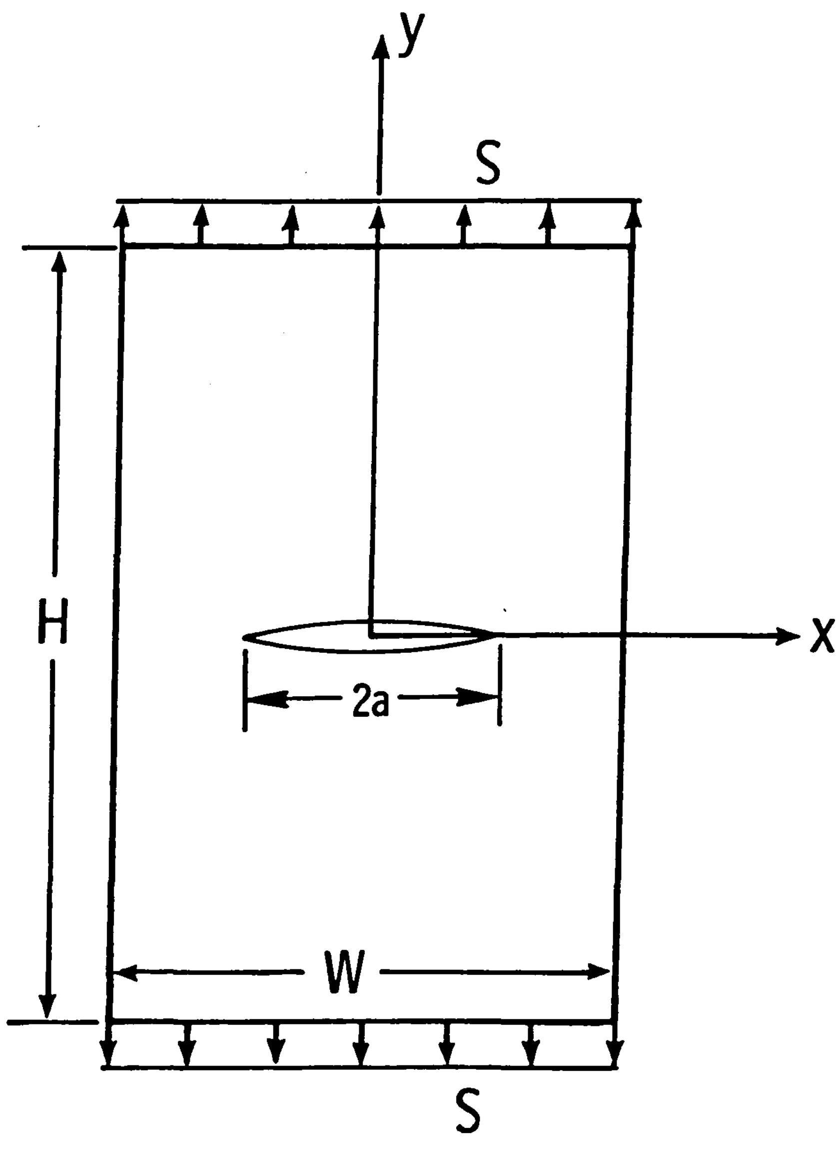

Figure 1 - Crack in finite plate subjected to unaxial tension.

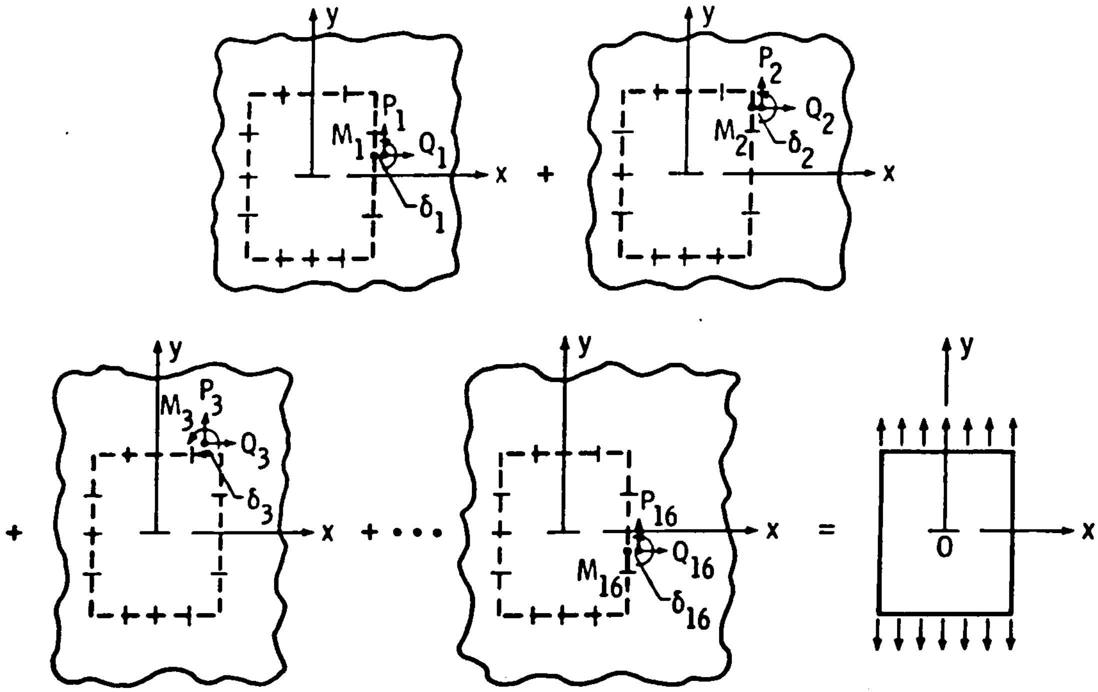

Figure 2 - Superposition of unknown forces P_i, Q_i and moment M_i on sixteen boundary segments (i = 1 to 16).

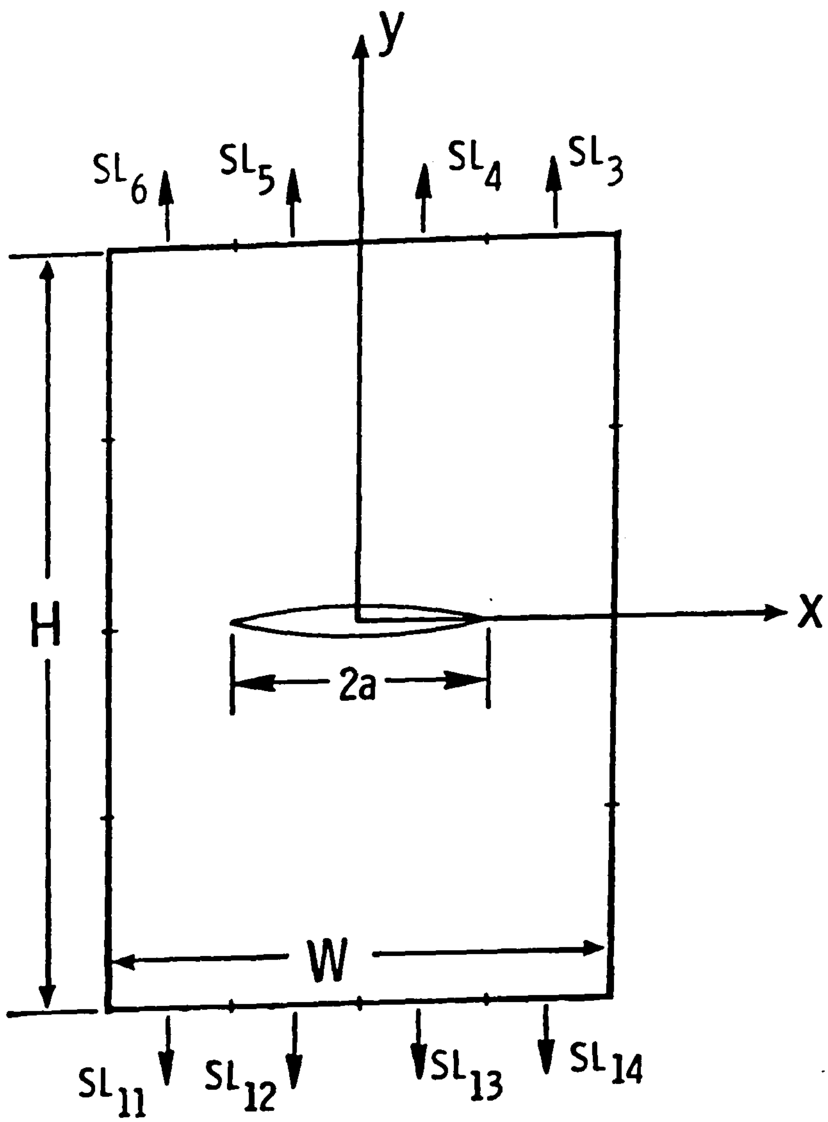

Figure 3 - Replacements of tractions by concentrated forces.

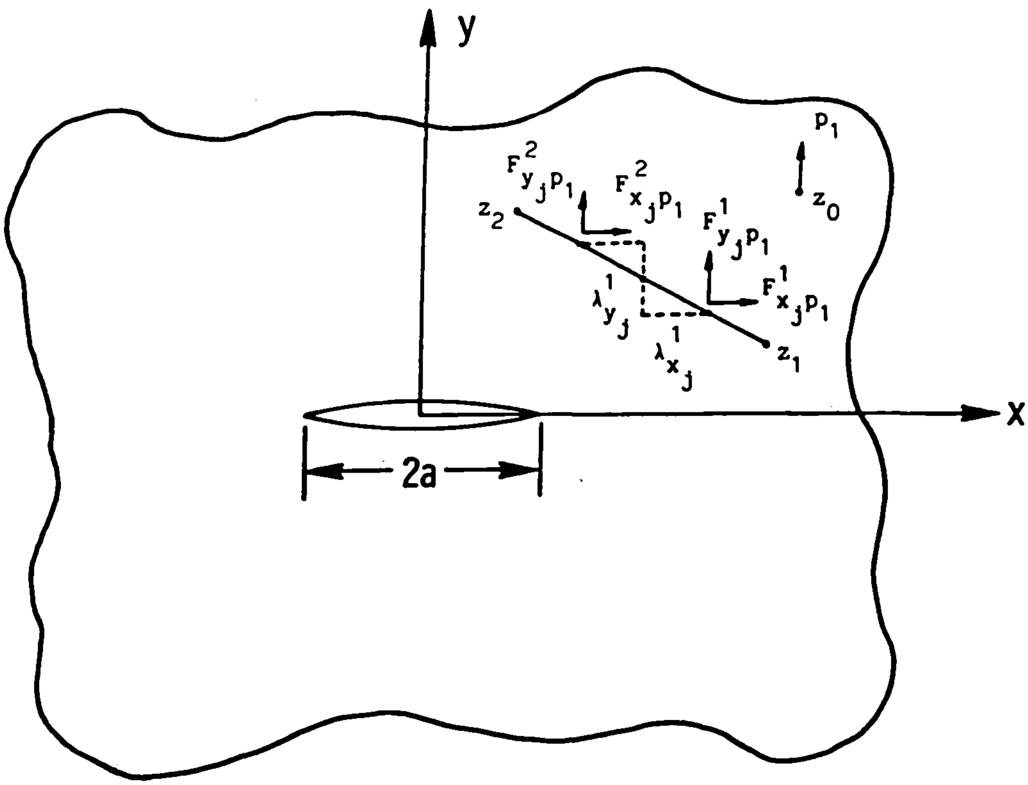

Figure 4 - Subdivision of a segment.

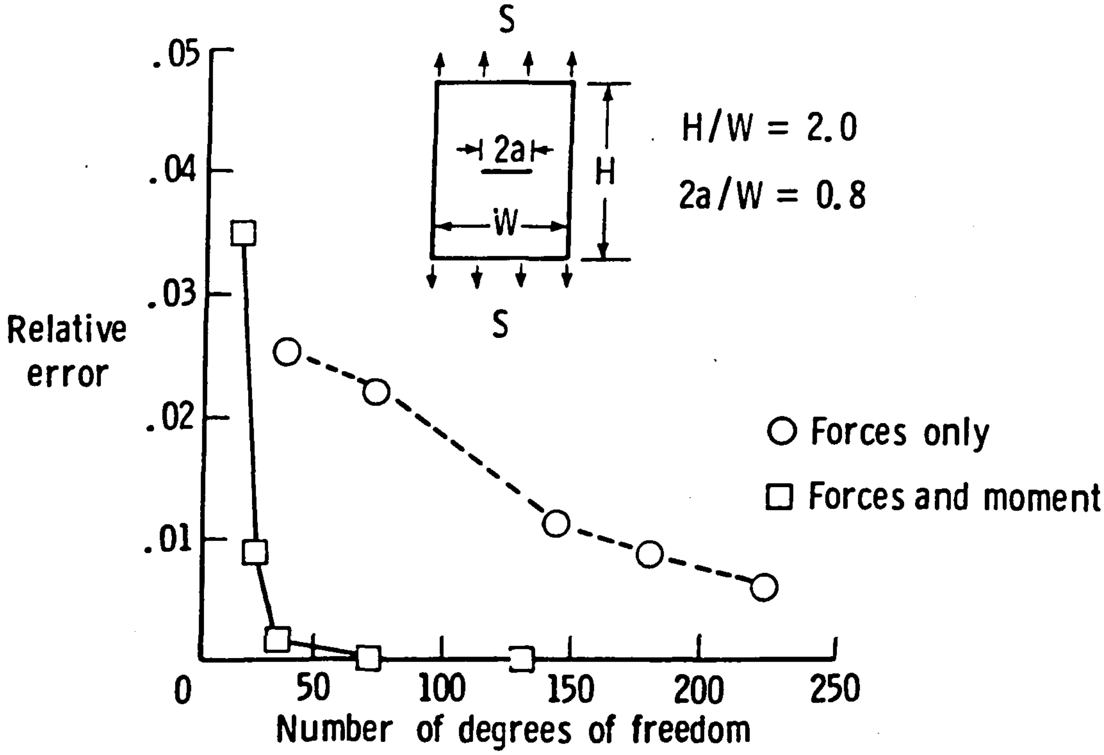

Figure 5 - Relative error in stress-intensity factor using either "force and moment" method or "force" method

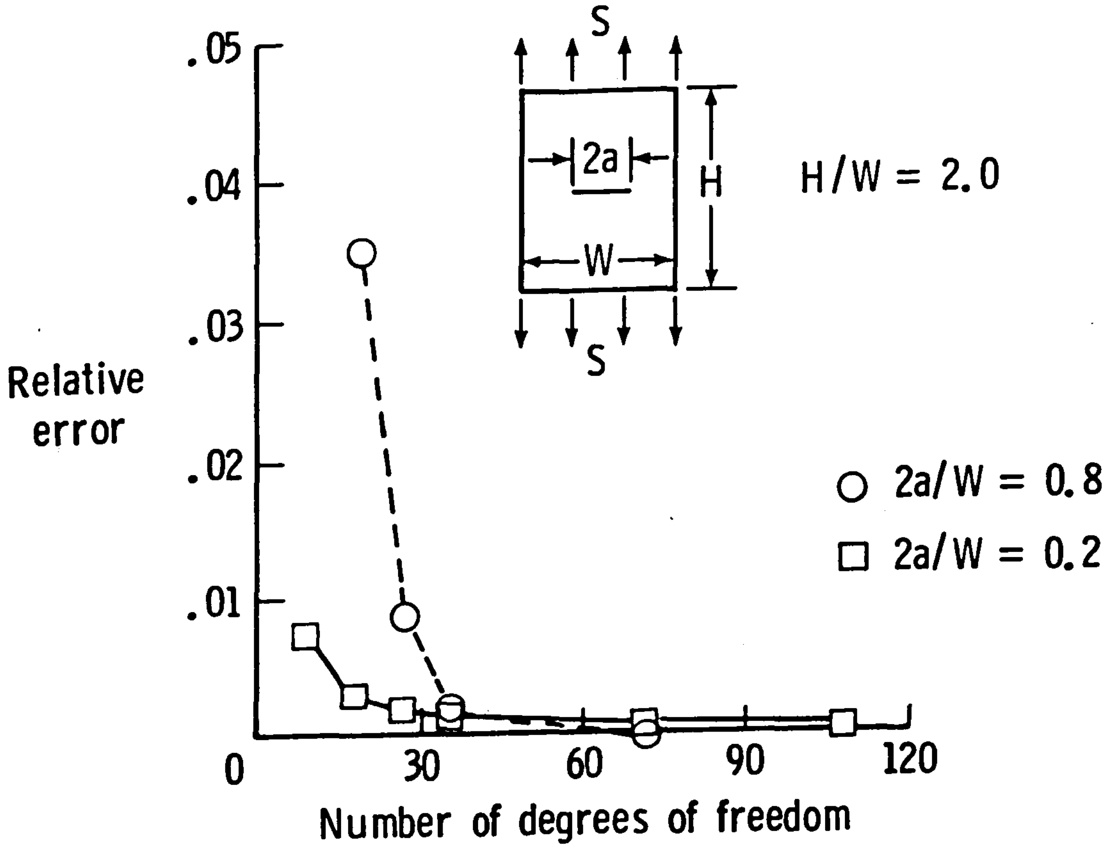

Figure 6 - Convergence of relative error in stress-intensity factor for center-crack tension specimen.

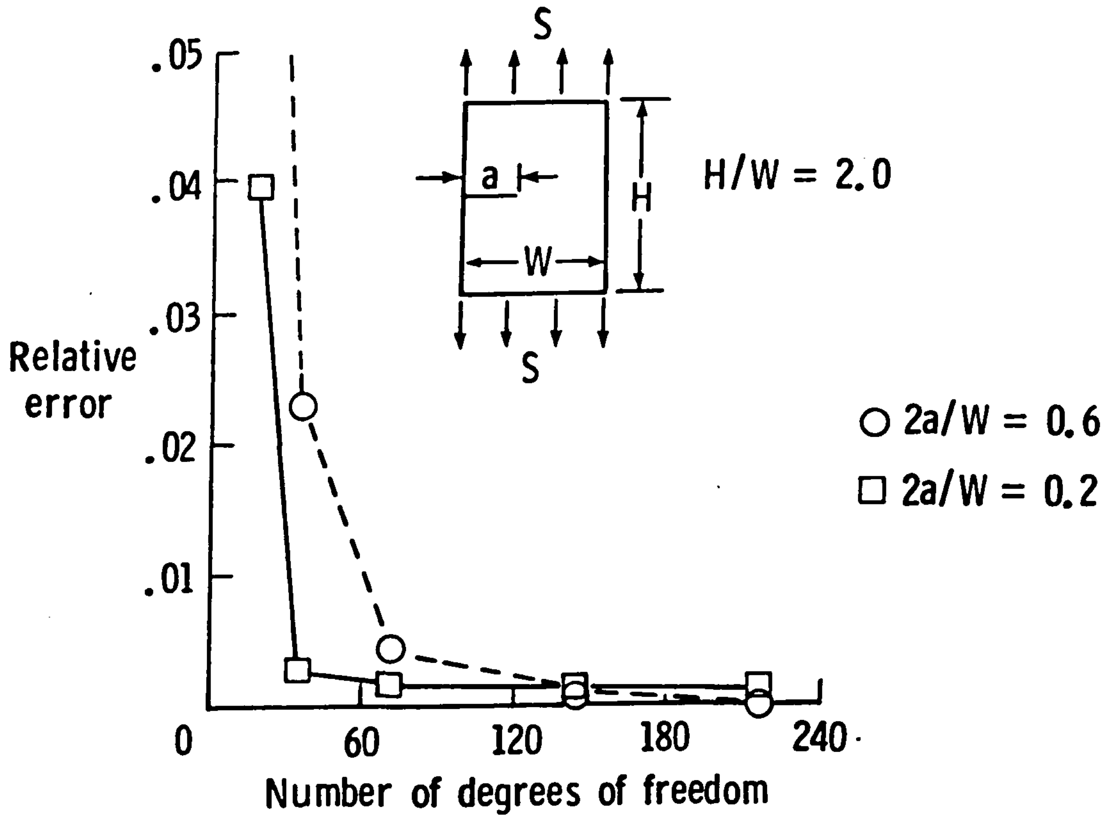

Figure 7 - Convergence of relative error in stress-intensity factor for single edge-crack tension specimen.

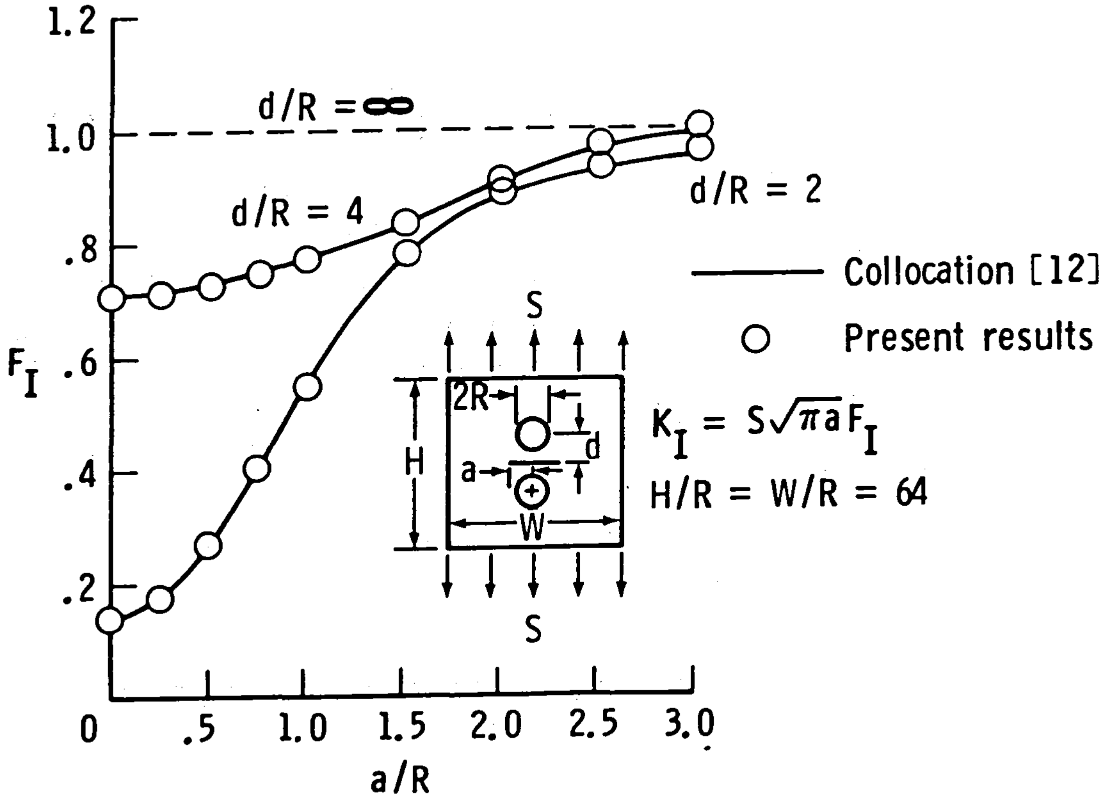

Figure 8 - Comparison of stress-intensity correction factors for a crack located between two holes.

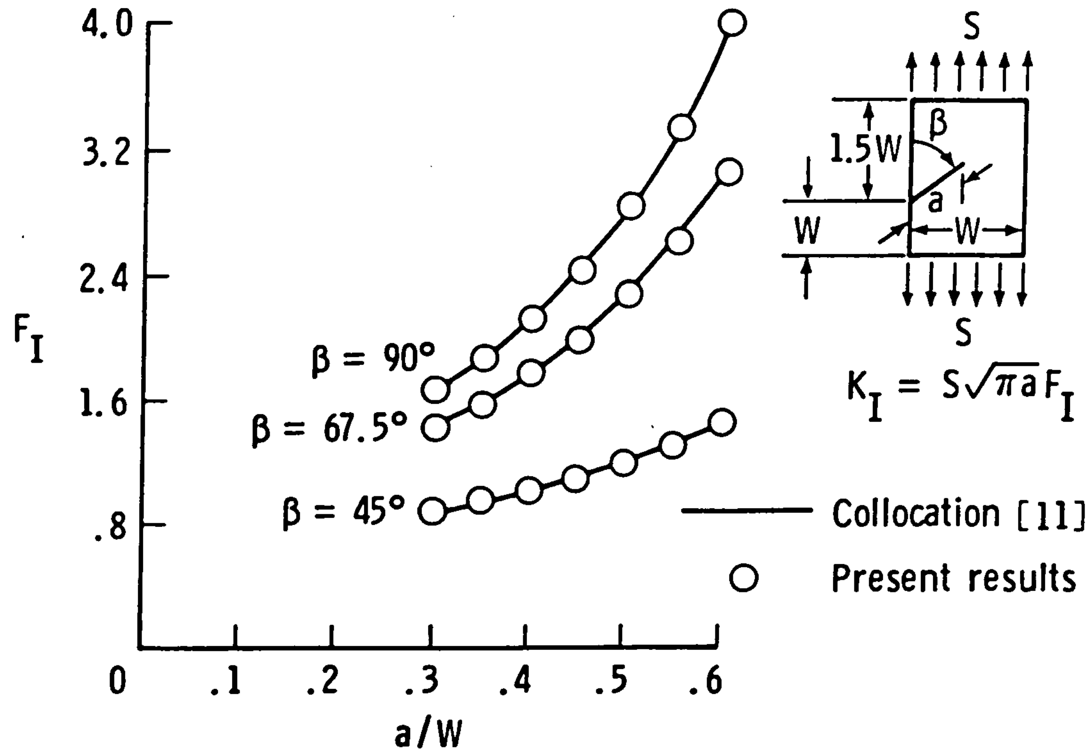

Figure 9 - Mode I stress-intensity correction factors for a slant single edge crack.

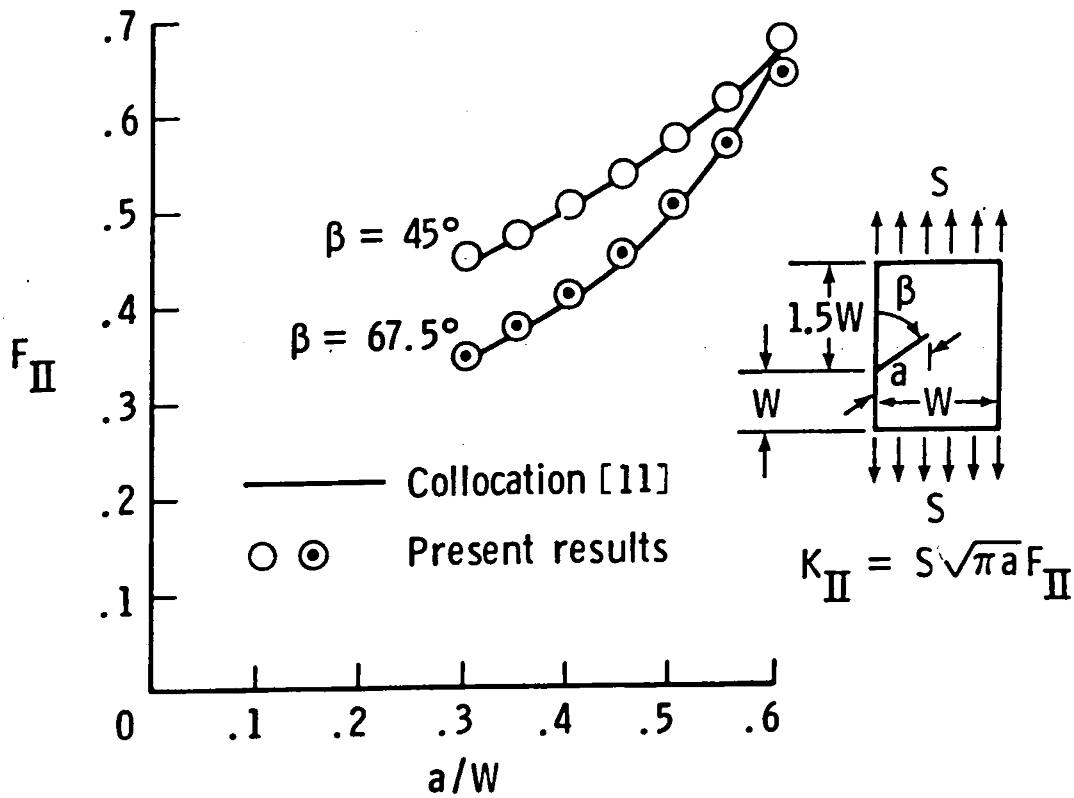

Figure 10 - Mode II stress-intensity correction factors for a slant single edge crack.

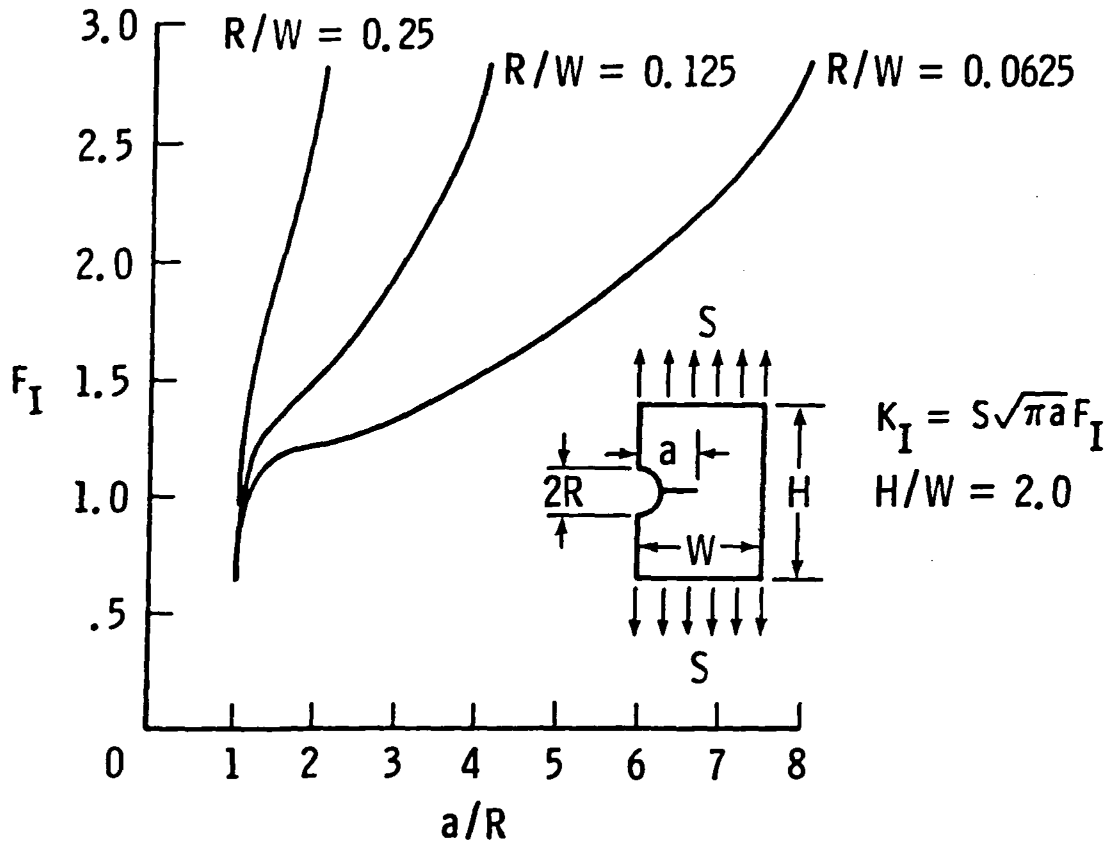

Figure 11 - Stress-intensity correction factors for an edge crack emanating from a semi-circular hole.

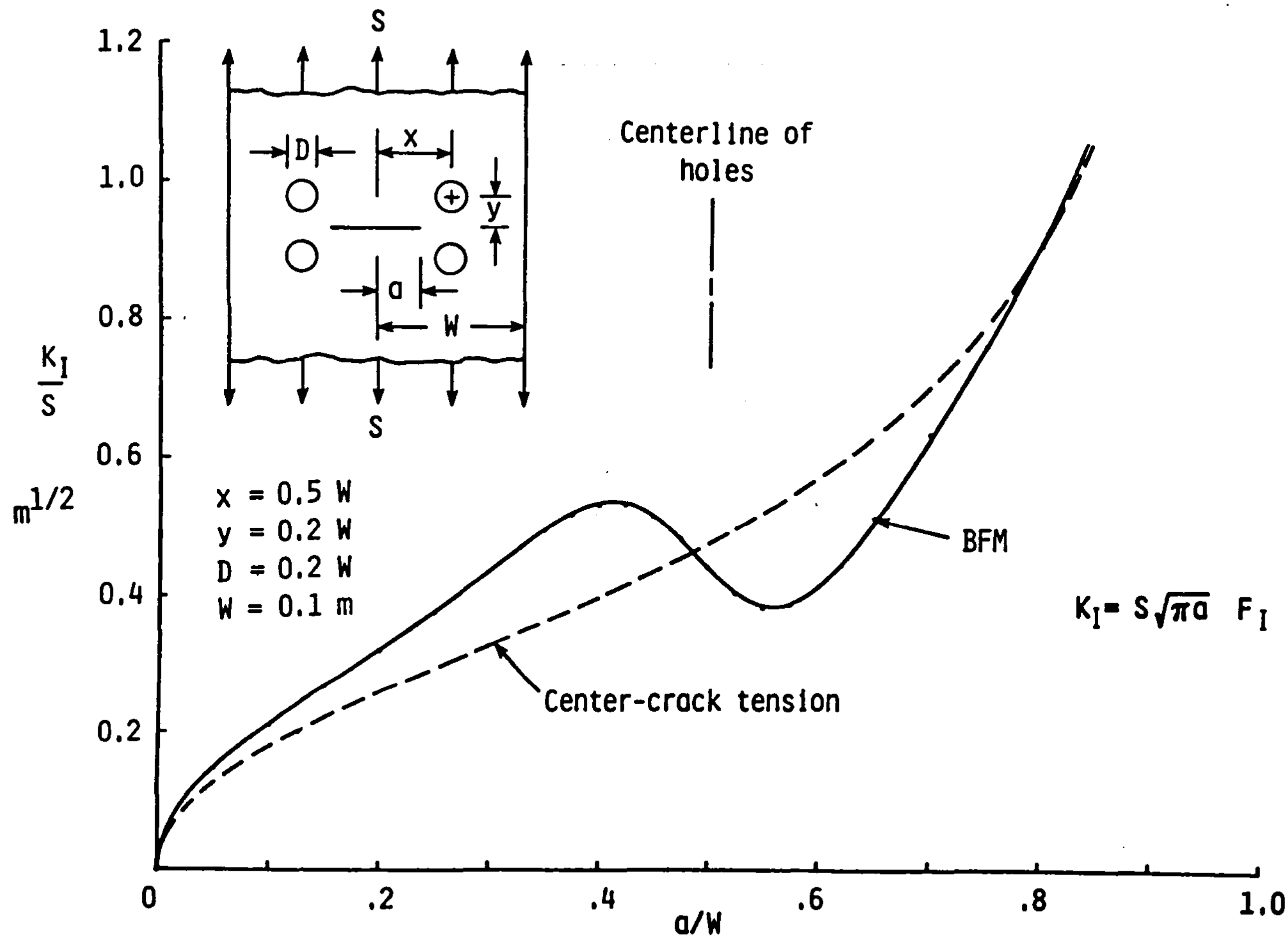

Figure 12 - Stress-intensity correction factor for a four-hole crack specimen.

Standard Bibliographic Page

1. Report No.	2. Government Accession No.	3. Recipient's Catalog No.
NASA TM-87725		

4. Title and Subtitle	5. Report Date
Boundary Force Method for Analyzing Two-Dimensional Cracked Bodies	May 1986
	6. Performing Organization Code 505-63-01
7. Author(s) P. W. Tan*, I. S. Raju* J. C. Newman, Jr.	8. Performing Organization Report No.
9. Performing Organization Name and Address NASA Langley Research Center Hampton, VA 23665-5225	10. Work Unit No.
	11. Contract or Grant No.
12. Sponsoring Agency Name and Address National Aeronautics and Space Administration Washington, DC 20546-0001	13. Type of Report and Period Covered Technical Memorandum
	14. Sponsoring Agency Code

15. Supplementary Notes

*P. W. Tan and I. S. Raju, Analytical Services & Materials, Inc., Hampton, VA

16. Abstract

The Boundary Force Method (BFM) was formulated for the two-dimensional stress analysis of complex crack configurations. In this method, only the boundaries of the region of interest are modeled. The boundaries are divided into a finite number of straight-line segments, and at the center of each segment, concentrated forces and a moment are applied. This set of unknown forces and moments are calculated to satisfy the prescribed boundary conditions of the problem. The elasticity solution for the stress distribution due to concentrated forces and a moment applied at an arbitrary point in a cracked infinite plate are used as the fundamental solution. Thus, the crack need not be modeled as part of the boundary.

The formulation of the BFM is described and the accuracy of the method is established by analyzing several crack configurations for which accepted stress-intensity factor solutions are known. The crack configurations investigated include mode I and mixed mode (mode I and II) problems. The results obtained are, in general, within ± 0.5 percent of accurate numerical solutions.

The versatility of the method is demonstrated through the analysis of complex crack configurations for which limited or no solutions are known.

17. Key Words (Suggested by Authors(s))	18. Distribution Statement
Cracks Stress-intensity factor Stress-concentration factor Stress functions Elasticity Holes	Unclassified - Unlimited Subject Category 39

19. Security Classif.(of this report)	20. Security Classif.(of this page)	21. No. of Pages	22. Price
Unclassified	Unclassified	43	A03

For sale by the National Technical Information Service, Springfield, Virginia 22161

NASA Langley Form 63 (June 1985)

End of Document